NANO LETTERS

2009
Vol. 9, No. 11
3940-3944

Direct Correlation between Structural and Optical Properties of III−V Nitride Nanowire Heterostructures with Nanoscale Resolution

Sung K. Lim,[†] Megan Brewster,[†] Fang Qian,[‡,⊥] Yat Li,[§] Charles M. Lieber,[‡,∥] and Silvija Gradečak*[,†]

Department of Materials Science and Engineering, Massachusetts Institute of Technology, Cambridge, Massachusetts 02139, Department of Chemistry and Chemical Biology, School of Engineering and Applied Sciences, Harvard University, Cambridge, Massachusetts 02138, and Department of Chemistry and Biochemistry, University of California, Santa Cruz, California 95064

Received August 6, 2009; Revised Manuscript Received August 28, 2009

ABSTRACT

Direct correlation of structural and optical properties on the nanoscale is essential for rational synthesis of nanomaterials with predefined structure and functionality. We study optical properties of single III−V nitride nanowire radial heterostructures with measured spatial resolution of <20 nm using cathodoluminescence (CL) technique coupled with scanning transmission electron microscopy (STEM). Enhanced carrier recombination in nanowire quantum wells and reduced light emission from regions containing structural defects were directly observed. Using newly developed parallel-detection-mode CL-STEM, we show that optical properties can vary within a single nanowire heterostructure as a function of nanowire morphology.

Nanostructured materials exhibit interesting size- and morphology-dependent properties and offer unique opportunities for fundamental studies and applications of light-matter interactions.[1−3] In particular, semiconductor nanowires and nanowire heterostructures have emerged as an important class of nanomaterials for applications in nanophotonics and optoelectronics. The optical excitation of single nanowire cavities have produced wavelength-tunable stimulated emission[4] and lasing with low lasing thresholds,[5] electrically injected light-emitting diodes have been demonstrated using radial[6] and axial[7] nanowire heterostructures, and axial nanowire heterostructures can act as single photon emitters.[8] Relevant electron energy levels in nanowire heterostructures are position dependent; consequently, nanowire device functionalities, such as emission wavelength and extraction efficiency, are sensitive to miniscule changes in interface quality and interdiffusion between nanowire segments or surface passivation layers. Only methods that combine a multitude of complementary techniques on the nanometer scale can provide direct insight into the complex structure-properties interplay within semiconductor nanowires, as well as in other nanostructured materials. Here, we show that scanning transmission electron microscopy (STEM) coupled with cathodoluminescence (CL) provides simultaneous structural, compositional, and optical information with high spatial resolution.

CL is a spectroscopic technique based on the light emission as a result of electronic excitation.[9] A highly focused electron beam generates electron−hole pairs within a sample, which diffuse and recombine through radiative or nonradiative processes. Far-field CL inside a scanning electron microscope (CL-SEM) is a common technique; but CL-STEM, although scarcely available, provides improved spatial resolution[9−11] due to small probe sizes, high electron energies, and thin samples, all of which decrease the beam-sample interaction volume (Supporting Information, Figure S1). Transmission electron microscopy (TEM) images and energy dispersive X-ray spectroscopy (EDS) maps can be recorded simultaneously with CL-STEM images providing complementary structural and chemical information. In this work, we have further advanced CL-STEM technique by enabling parallel-detection imaging (Figure 1) for the first time; the electron

* To whom correspondence should be addressed. E-mail: gradecak@mit.edu.
[†] Massachusetts Institute of Technology.
[‡] Department of Chemistry and Chemical Biology, Harvard University.
[§] University of California.
[∥] School of Engineering and Applied Sciences, Harvard University.
[⊥] Present address: Department of Molecular, Cellular, and Developmental Biology, University of California, Santa Barbara, California 93106.

10.1021/nl9025743 CCC: $40.75
Published on Web 09/23/2009

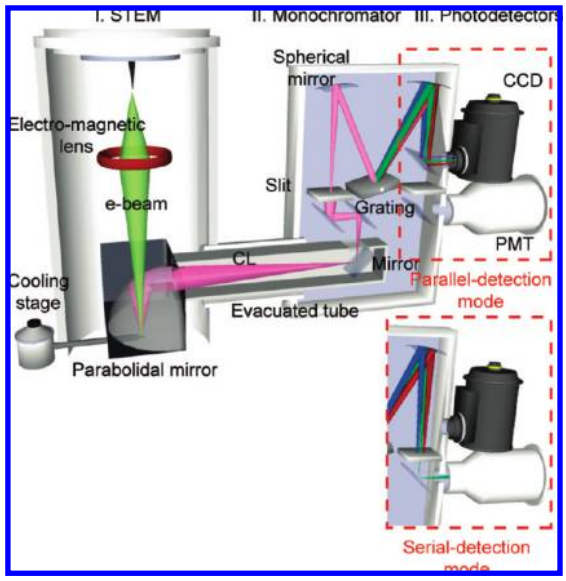

Figure 1. Schematic drawing of our CL-STEM setup. The electron beam is converged into a ~1 nm spot size onto a thin TEM sample. Locally generated CL light is collected by a paraboloidal-shaped mirror placed inside the STEM column directly above the sample and then transmitted through an evacuated tube to the monochromator. In parallel-detection-mode, the dispersed light is directed by two mirrors into a charge-coupled device (CCD) and three-dimensional data set $I(x,y,\lambda)$ is acquired as the beam scans across the sample. In serial-detection-mode, the reflected light is filtered by a slit and then detected by a photomultiplier tube (PMT) to form monochromatic images or CL spectra. The sample is mounted on the nitrogen cryogenic TEM holder to control the sample temperature.

beam is scanned in an *x*-*y* pattern and emission spectra are measured at each point, generating a three-dimensional "hyperspectral" data set $I(x,y,\lambda)$. Because the complete spectroscopic information is collected in a single electron-beam scan, the parallel detection minimizes effects of electron-beam damage that can inhibit multiple or more complex CL studies of a single nano-object.

The main parts of our CL-STEM are depicted in Figure 1; the JEOL 2011 TEM/STEM was equipped with a Gatan MonoCL3 CL+ system consisting of a retractable collection mirror and a light guide, a monochromator, and photodetectors. In STEM mode, the emitted electron-beam is converged and either kept at one position or scanned over the sample. Emitted CL light is collected by a paraboloidal-shaped mirror (~3 mm in height) above the sample and is passed through an evacuated tube to the monochromator. By adjusting a pivoting mirror, the light can be analyzed by either a charge-coupled device (CCD) or photomultiplier tube (PMT) for parallel- or serial-detection-modes, respectively. In the parallel-detection-mode, the light is dispersed onto the 1340 × 100 pixel CCD and the whole CL spectrum is detected simultaneously for each (x,y) position of the sample. In the serial-detection-mode, a specific wavelength is selected by a slit and its intensity is recorded by the PMT to produce monochromatic intensity maps of the sample. For CL experiments, a low accelerating voltage of 120 kV was used to minimize the sample damage from electron beam radiation. Sample temperature was controlled by a liquid nitrogen-cooled cryogenic holder in the range of 110−300 K. Bright field and lattice-resolved images were studied by a JEOL 2010F field-emission TEM operating at 200 kV and compositional characterization by accompanying EDS detector.

We concentrate on CL-STEM studies of (Al,Ga,In)N radial nanowire heterostructures because of their attractive properties, that is, bandgap tunability from ultraviolet to infrared and dislocation-free structures that reduce the number of scattering centers and nonradiative exciton recombination centers typically encountered in their thin film counterparts.[12] All nanowires reported in this study were grown by metalorganic chemical vapor deposition (MOCVD), as previously reported.[6,13] First, we investigated the overall optical properties of individual GaN/AlGaN core−shell (CS) nanowires. In this relatively simple nanowire heterostructure, GaN core acts as an active light emission region, while the AlGaN shell prevents nonradiative surface recombination of carriers. A bright field plan-view TEM image with associated selected area diffraction (SAD) pattern and lattice-resolved image of a representative GaN/AlGaN nanowire (Figure 2a) reveal that the CS nanowire grew along the [11-20] direction with a single-crystalline wurtzite structure. An EDS linescan performed across the nanowire (Figure 2b) shows distinct spatial profiles of Al and Ga, confirming that an AlGaN shell encapsulates the GaN core. EDS Al and Ga profiles tightly fit the model of a CS nanowire with the overall triangular cross-section that consists of one {0001} and two {1-101} facets and with a GaN core with truncated corners consisting of {0001}, {1-101}, and {1-100} facets (Supporting Information, Figure S2). Observed variations in the shape of the nanowire cross-section before and after the shell deposition can be attributed to different facet stabilities under various growth conditions (core vs shell growth).[14]

Figure 2c shows temperature-dependent CL spectra of the same nanowire. At room temperature, the CL spectrum shows a main peak centered at 365 nm (3.40 eV), corresponding to the GaN near-band-edge (NBE) emission,[5,15] and no emission from the AlGaN shell was observed. As the sample was cooled, NBE intensity gradually decreased and its wavelength blueshifted by approximately 40 meV from room temperature to 150 K. Simultaneously, at 200 K a longer wavelength peak emerged at 380 nm (3.26 eV) and eventually dominated the spectrum. At 110 K, this peak is positioned at 378 nm (3.28 eV) and can be indexed as donor−acceptor pair (DAP) emission[16] with associated longitudinal optic phonon replicas also resolved (Supporting Information, Figure S3). The observed redshift of the DAP transition at higher temperatures can be explained by either Varshini's law or donor ionization[16] and future studies with higher spectral resolution and narrower temperature variation will concentrate on identifying the source of the shift. DAP emission indicates the presence of acceptor impurities or defects such as Si_N[17] or V_{Ga}-O complex[16] in the Si-doped GaN core, and the observed transition from DAP to NBE at higher temperatures is most likely due to quenching of the internal quantum efficiency of DAP emission compared to that of NBE.[18] Spatial distribution of the CL emission investigated using monochromatic CL mapping at 365 nm

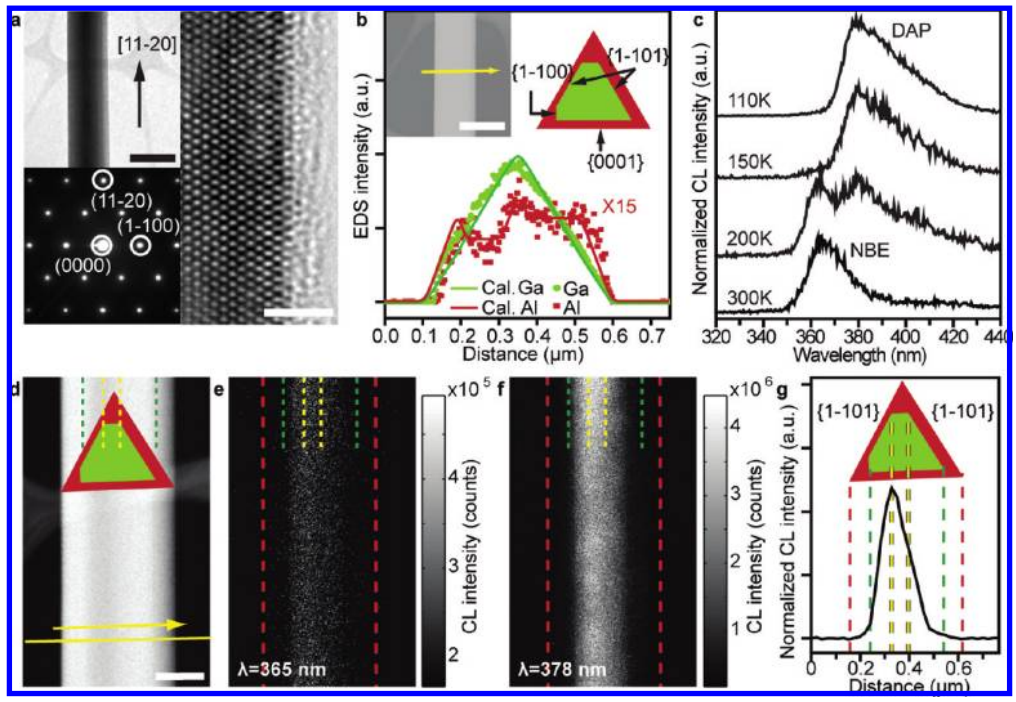

Figure 2. Microstructure and optical properties of a single GaN/AlGaN CS nanowire. (a) Low-magnification bright-field TEM image of a CS nanowire taken along [0001] zone axis (top-left, the scale bar is 500 nm) and corresponding SAD pattern (bottom-left) indicating the growth direction of the nanowire is [11-20]. Lattice-resolved TEM image of the CS nanowire taken along [0001] zone axis (right), the scale bar is 2 nm. (b) Experimental EDS linescan profile of Al (red squares) and Ga (green circles) acquired across the CS nanowire. Position and the scan direction are depicted by the yellow arrow in the dark-field STEM image (top-left). The scale bar is 500 nm. EDS profiles of Al and Ga were fitted (red and green solid lines, respectively) with the model consisting of pentagonal shaped GaN core and triangular shaped AlGaN shell with different shell thickness on each facet, schematically shown in top-right (for more information, see Supporting Information, Figure S2). (c) Normalized CL spectra of the same nanowire taken at different temperatures showing NBE emission at the room temperature and development of DAP emission at lower temperatures. Spectra are offset for clarity. (d) Dark-field STEM image with an overlaid schematic drawing of CS structure obtained by the EDS model. STEM image was taken at approximately 2° from the [0001] zone axis. Red, green, and yellow dashed lines indicate the outline of the CS nanowire, the interface between GaN and AlGaN, and the outline of the {0001} core facet, respectively. The scale bar is 200 nm. (e,f) Monochromatic CL images at 365 nm (recorded at 300 K) and at 378 nm (recorded at 110 K). Both monochromatic images were taken in the same region as (d) with identical dashed line overlays and under the identical acquisition parameters, except for temperature. (g) Normalized CL intensity profile of the 378 nm DAP emission taken along the yellow line indicated in (d). The scheme outlines the nanowire orientation along the electron beam.

at room temperature and 378 nm at 110 K (Figure 2e,f, respectively) further demonstrates that both NBE and DAP emissions originate from the GaN core, implying overall uniform distribution of dopants throughout the core with small intensity variations observed on the submicrometer scale that is likely due to sample morphology variations or surface trapping states. Interestingly, the intensity profile of the DAP emission (Figure 2g) is proportional to the projected thickness of the nanowire core along the beam direction but with emission quenched at the nanowire corners. The quenching can be caused by piezo-electric and spontaneous polarization of AlGaN shell, which induce charge separation[19] and thus reduce the probability of radiative recombination near the GaN/AlGaN interface, which is mostly pronounced at the nanowire corners.

We further studied more complex single quantum well (SQW) nanowire radial heterostructures (GaN/InGaN/GaN/AlGaN). First, we will concentrate on cross-section CL imaging to investigate structure and optical properties of individual heterostructure layers. The bright field image and associated SAD pattern (Figure 3a) allow indexing of the facets of the triangular nanowire cross-section with one {0001} and two {1-101} facets. A STEM image (Figure 3b) shows a thin (~4 nm) InGaN SQW on {1-101} facet, but no InGaN contrast was observed on the {0001} facet. EDS linescan (Figure 3c) further confirmed that no InGaN growth occurred on the {0001} facet, while the AlGaN shell was deposited on all nanowire facets. InGaN has been reported to have different growth rates depending on the deposition planes,[20] which might explain the selective growth on {1-101} nanowire facets. The distinct EDS linescans for Al and In suggest that no interdiffusion of In and Al took place across individual shells. On the basis of these results, the model of the nanowire heterostructure was developed (Figure 3d).

Optical properties of the same SQW cross-sectional sample were analyzed by CL-STEM. CL spectrum collected at 110 K (Figure 3f) has two main peaks centered at 378 nm (3.28 eV) and 430 nm (2.88 eV). The first peak is again attributed to the GaN DAP emission, while the second peak indicates presence of $In_xGa_{1-x}N$ with $x \approx 0.14$.[21] Interestingly, monochromatic imaging shows distinct spatial distribution of the two peaks; the DAP emission originates only from the GaN core (Figure 3g), while the emission at 430 nm is localized at the edges of {1-101} facets (Figure 3h), consistent with the presence of InGaN QWs. The monochromatic CL image

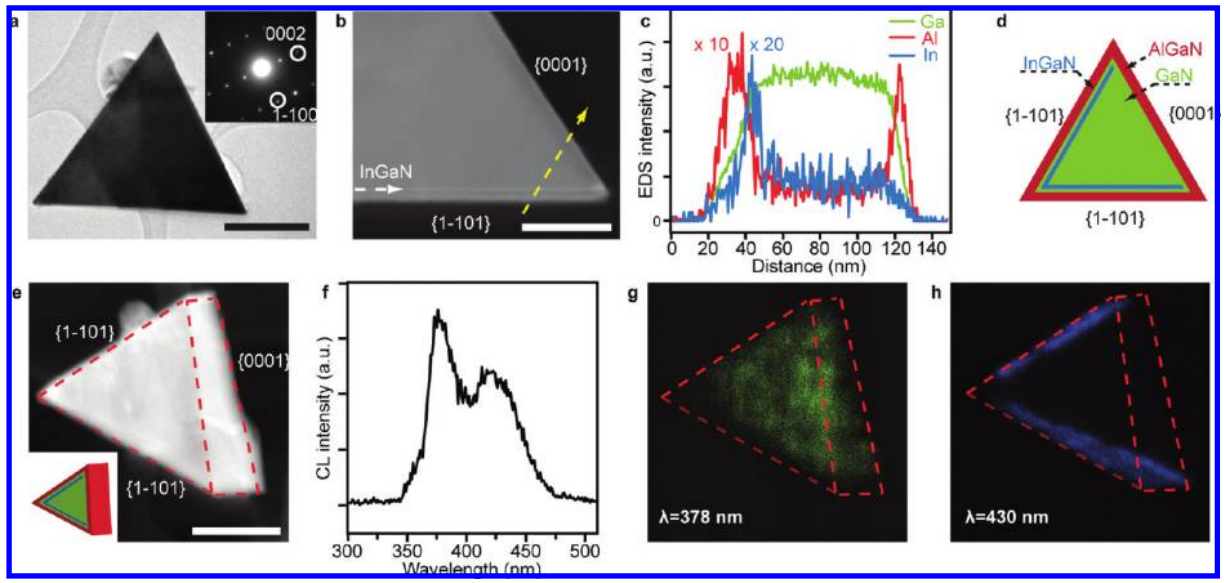

Figure 3. Direct correlation between structural and optical properties of a GaN/InGaN/GaN/AlGaN SQW nanowire. (a) Cross-sectional bright-field TEM image and corresponding SAD pattern of the SQW nanowire taken along the [11-20] zone axis. The scale bar is 300 nm. (b) Dark-field STEM image at the corner of {1-101} and {0001} facets. The bright line along the {1-101} facet pointed out by white dashed arrow indicates presence of InGaN SQW due to the atomic mass contrast. The scale bar is 100 nm. (c) EDS linescan profiles of Al, Ga, and In in direction of a dashed yellow arrow in (b). For clarity, Al and In EDS signals are multiplied by 10 and 20, respectively. (d) Cross-section schematic drawing of the SQW nanowire based on STEM and EDS results. (e) Dark-field STEM image of the same SQW nanowire during the CL measurement. The nanowire is off the [11-20] zone axis by ~15° (schematically shown in the inset). Red dashed line indicates the outline of the cross-sectional sample. The scale bar is 300 nm. (f) CL spectrum of the SQW nanowire, obtained at 110 K from the same region as (e). Monochromatic images at 378 (g) and 430 nm (h) with red dashed line indicating the outline of the sample. Monochromatic images were taken in the same region as in (e), with identical scale.

at 430 nm also shows the reduced intensity in the corner of the two {1-101} facets, which is likely due to structural imperfections observed in this region (Supporting Information, Figure S4).[4] We directly measure the spatial resolution of the CL signal to be less than 20 nm, based on the full-width at half-maximum of the CL intensity profile for the nanowire SQW (Supporting Information, Figure S5). This resolution is comparable or better than the best resolution of fluorescence near-field scanning optical microscopy[22] and low-voltage CL-SEM,[23] both of which are limited to surface studies. Our results indicate that CL-STEM resolution can be further improved by optimizing the sample thickness and geometry.

While the cross-sectional CL-STEM studies of nanowire heterostructures provide a wealth of information, these concentrate on a thin slice obtained from a particular nanowire position. Therefore, we used parallel-detection CL-STEM to investigate the influence of overall nanowire morphology on optical properties of a single GaN/InGaN/GaN/AlGaN SQW nanowire with nonuniform (tapered) diameter (Figure 4a). Figure 4b shows a hyperspectral CL image taken along the nanowire length. Notably, several spectral features were observed; DAP emission from the nanowire core was fixed at 378 nm, while three distinct CL peaks recorded at longer wavelengths experienced strong redshift as the thickness of the nanowire increased (Figure 4c). Because GaN DAP emission is consistent along the axial nanowire direction, longer wavelength peaks were attributed to distinct InGaN layers on different nanowire facets with varying thickness and/or composition along the nanowire length causing the observed redshift and relative intensity variations (Figure 4b). Continuous thickness[24] and compositional[25] variations in III−V CS nanowires have been previously reported and can be associated to the difference in the arrival rates of growth species during MOCVD growth. Raman spectroscopy results (not shown) support the CL findings, showing that at least two InGaN compositions coexist in the nanowire with increasing In concentration and increasing volume (thicker nanowire shell) as the nanowire thickness increases; both of these effects can cause redshift of the CL emission. Multiple cross-section CL maps from slices obtained along the nanowire length will be a powerful tool for studies of quantum well evolution in nanowire heterostructures and III−V nitride systems in general.

Our results provide direct insight into optical properties of single nanowire heterostructures in direct correlation with their structure. A collection of complex spectroscopic information is enabled by the parallel CL detection in a single electron-beam scan, which minimizes electron-beam sample damage.[26] Cross-section CL images illustrate the rich complexity of GaN-based nanowire heterostructures and offer a platform for basic growth studies in nitride systems. Plan-view CL images show that nanowire properties can vary within a single nanowire, underlining the importance of future studies to achieve uniformity of nanowire properties, for example through nanowire density control.[27,28] Finally, detection of DAP emission in our nanowires proves that the CL technique can be sensitive to small concentrations of impurities that are too low to be detected using EDS or electron energy loss spectroscopy. Parallel-detection-mode

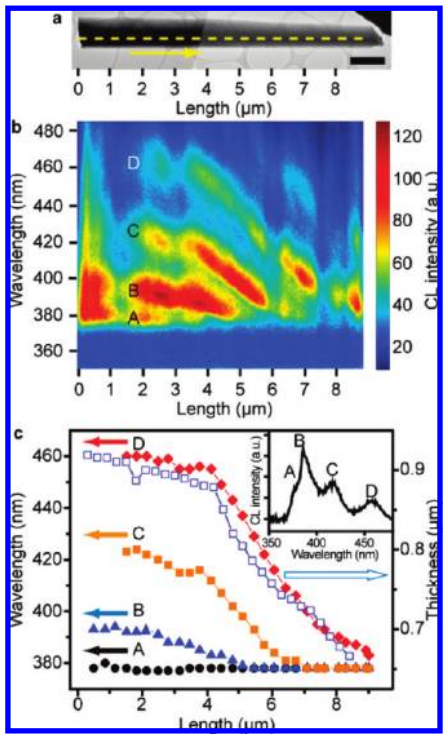

Figure 4. CL properties of a SQW nanowire with nonuniform (tapered) diameter. (a) Bright field TEM image of a tapered SQW nanowire. The scale bar is 1 μm. (b) CL linescan along the yellow dashed line in (a) along the direction indicated by the arrow, taken at 110 K. CL emission intensity is graphed as a function of the wavelength and emission position along the linescan and four distinct peaks are labeled as A, B, C, and D. Relative intensities of the peaks change along the nanowire length, while discrete CL intensity dips were observed due to the light absorption by the lacey carbon[29] above the nanowire. This sample geometry was selected to position the nanowire in the focal point of the collection mirror and maximize the CL signal. (c) Wavelength of multiple emission peaks (left *y*-axis) and thickness variation along the nanowire length (right *y*-axis). Solid symbols with different colors represent the center wavelengths of multiple emissions (A, B, C, and D in (b)) and blue hollow symbol represents the thickness variation along the nanowire. Inset shows a single CL spectrum extracted from the hyperspectral image (b) at the position of 3.5 μm. Peak position A remains approximately constant, whereas peaks B, C, and D show redshift as the sample thickness increases.

CL, combined with the directly measured CL-STEM spatial resolution of <20 nm, bridges the gap that exists between high-resolution imaging and direct structure−property correlation, giving way to a new realm of nanoscale characterization.

Acknowledgment. This work was supported in part by the MRSEC Program of the National Science Foundation under award number DMR-0213282, Interconnect Focus Center, and NSF CAREER award DMR-0745555 (S.G.), and by the Air Force Office of Scientific Research (C.M.L.). We thank Dr. Yong Zhang, Dr. Anthony Garratt-Reed, and Arthur Reading for their technical support.

Supporting Information Available: Simulated and measured spatial resolution of cathodoluminescence in scanning transmission electron microscopy; structural analysis of GaN/AlGaN and GaN/InGaN/GaN/AlGaN nanowire heterostructures; Donor−acceptor-pair emission and phonon replicas in a GaN/AlGaN nanowire. This material is available free of charge via the Internet at http://pubs.acs.org.

References

(1) Li, Y.; Qian, F.; Xiang, J.; Lieber, C. M. *Mater. Today* **2006**, *9* (10), 18–27.
(2) Yoffe, A. D. *Adv. Phys.* **2001**, *50* (1), 1–208.
(3) Pauzauskie, P. J.; Yang, P. *Mater. Today* **2006**, *9* (10), 36–45.
(4) Qian, F.; Li, Y.; Gradečak, S.; Park, H. G.; Dong, Y. J.; Ding, Y.; Wang, Z. L.; Lieber, C. M. *Nat. Mater.* **2008**, *7* (9), 701–706.
(5) Gradečak, S.; Qian, F.; Li, Y.; Park, H. G.; Lieber, C. M. *Appl. Phys. Lett.* **2005**, *87* (17), 173111.
(6) Qian, F.; Gradečak, S.; Li, Y.; Wen, C. Y.; Lieber, C. M. *Nano Lett.* **2005**, *5* (11), 2287–2291.
(7) Minot, E. D.; Kelkensberg, F.; van Kouwen, M.; van Dam, J. A.; Kouwenhoven, L. P.; Zwiller, V.; Borgstrom, M. T.; Wunnicke, O.; Verheijen, M. A.; Bakkers, E. *Nano Lett.* **2007**, *7* (2), 367–371.
(8) Borgstrom, M. T.; Zwiller, V.; Muller, E.; Imamoglu, A. *Nano Lett.* **2005**, *5* (7), 1439–1443.
(9) Yacobi, B. G.; Holt, D. B. *Cathodoluminescence microscopy of inorganic solids*; Plenum Press: New York, 1990.
(10) Spence, J. C. H. *High-resolution electron microscopy*; Oxford University Press: New York, 2003.
(11) Salviati, G.; Rossi, F.; Armani, N.; Grillo, V.; Lazzarini, L. Power-dependent cathodoluminescence in III-V ntrides heterostructures: from internal field screening to controlled band-gap modulation. In *Characterization of Semiconductor Heterostructures and Nanostructures*; Lamberti, C., Ed.; Elsevier: New York, 2008; pp 209−248.
(12) Jiang, D. S.; Zhao, D. G.; Yang, H. *Phys. Status Solidi B* **2007**, *244* (8), 2878–2891.
(13) Li, Y.; Xiang, J.; Qian, F.; Gradečak, S.; Wu, Y.; Yanv, H.; Yan, H.; Blom, D. A.; Lieber, C. M. *Nano Lett.* **2006**, *6* (7), 1468–1473.
(14) Hiramatsu, K.; Nishiyama, K.; Onishi, M.; Mizutani, H.; Narukawa, M.; Motogaito, A.; Miyake, H.; Iyechika, Y.; Maeda, T. *J. Cryst. Growth* **2000**, *221*, 316–326.
(15) Oh, E.; Choi, J. H.; Seong, H.-K.; Choi, H.-J. *Appl. Phys. Lett.* **2006**, *89*, 092109.
(16) Paskova, T.; Arnaudov, B.; Paskov, P. P.; Goldys, E. M.; Hautakangas, S.; Saarinen, K.; Sodervall, U.; Monemar, B. *J. Appl. Phys.* **2005**, *98* (3), 033508.
(17) Glaser, E. R.; Freitas, J. A.; Shanabrook, B. V.; Koleske, D. D.; Lee, S. K.; Park, S. S.; Han, J. Y. *Phys. Rev. B* **2003**, *68* (19), 195201.
(18) Reshchikov, M. A.; Korotkov, R. Y. *Phys. Rev. B* **2001**, *64* (11), 115205.
(19) Heikman, S.; Keller, S.; Wu, Y.; Speck, J. S.; DenBaars, S. P.; Mishra, U. K. *J. Appl. Phys.* **2003**, *93* (12), 10114–10118.
(20) Nishizuka, K.; Funato, M.; Kawakami, Y.; Fujita, S.; Narukawa, Y.; Mukai, T. *Appl. Phys. Lett.* **2004**, *85* (15), 3122–3124.
(21) Wu, J.; Walukiewicz, W.; Yu, K. M.; Ager, J. W.; Haller, E. E.; Lu, H.; Schaff, W. J. *Appl. Phys. Lett.* **2002**, *80* (25), 4741–4743.
(22) Gerton, J. M.; Wade, L. A.; Lessard, G. A.; MA, Z.; Quake, S. R. *Phys. Rev. Lett.* **2004**, *93* (18), 180801.
(23) Norman, C. E. *Microsc. Anal.* **2002**, *88*, 9–12.
(24) Lim, S. K.; Tambe, M. J.; Brewster, M. M.; Gradečak, S. *Nano Lett.* **2008**, *8* (5), 1386–1392.
(25) Kim, Y.; Joyce, H. J.; Gao, O.; Tan, H. H.; Jagadish, C.; Paladugu, M.; Zou, J.; Suvorova, A. A. *Nano Lett.* **2006**, *6* (4), 599–604.
(26) We observe that the overall CL intensity decreases during long electron beam irradiation such that some nanowires become optically inactive after multiple electron beam scans. A qualitative analysis of the electron beam effects will be a focus of our future studies.
(27) Tambe, M. J.; Lim, S. K.; Smith, M. J.; Allard, L. F.; Gradečak, S. *Appl. Phys. Lett.* **2008**, *93* (15), 151917.
(28) Borgström, M. T.; Immink, G.; Ketelaars, B.; Algra, R.; Bakkers, E. P. A. M. *Nat. Nanotechnol.* **2007**, *2*, 541–544.
(29) Savvides, N. *J. Appl. Phys.* **1986**, *59* (12), 4133–4145.

NL9025743